Coherence between two coupled lasers from a dynamics perspective

Will Ray,[1*] Jeffrey L. Rogers,[2] and Kurt Wiesenfeld[1]

[1]*Center for Nonlinear Science and School of Physics Georgia Institute of Technology, Atlanta, GA 30332-0430*

[2]*Control and Dynamical Systems, California Institute of Technology, Pasadena, CA 91125*

willray@gatech.edu

Abstract: We compare a simple dynamical model of fiber laser arrays with independent experiments on two coupled lasers. The degree of agreement with experimental observations is excellent. Collectively the evidence presented supports this dynamical approach as an alternative to the traditional static eigenmode analysis of the coupled laser cavities.

OCIS codes: (060.2320) Fiber optics amplifiers and oscillators; (140.3290) Laser arrays; (190.3100) Instabilities and chaos.

References and links

1. A. Liem, H. Limpert, and A. Tünnermann, "100W single-frequency master-oscillator fiber power amplifier," Opt. Lett. **28**, 1539 (2003).
2. P. Cheo, A. Liu, and G. King, "A high-brightness laser beam from a phase-locked multicore Yb-doped fiber laser array," IEEE Photon. Technol. Lett. **13**, 439–441 (2001).
3. E. Bochove, P. Cheo, and G. King, "Self-organization in a multicore fiber laser array," Opt. Lett. **28**, 1200–1202 (2003).
4. C. Corcoran and F. Durville, "Experimental demonstration of a phase-locked laser array using a self-Fourier cavity," Appl. Phys. Lett. **86**, 201,118 (2005).
5. V. Apollonov, S. Derzhavin, V. Kislov, V. Kuzminov, D. Mashkovsky, and A. Prokhorov, "Phase-locking of the 2D structures," Opt. Express **4**, 19–26 (1999).
6. M. Wrage, P. Glas, and M. Leitner, "Combined phase locking and beam shaping of a multicore fiber laser by structured mirrors," Opt. Lett. **26**, 980–982 (2001).
7. N. Lyndin, V. Sychugov, A. Tikhomirov, and A. Abramov, "Laser system composed of several active elements connected by single-mode couplers," Quantum Electron. **24**, 1058–1061 (1994).
8. V. Kozlov, J. Hernàndez-Cordero, and T. Morse, "All-fiber coherent beam combining of fiber lasers," Opt. Lett. **24**, 1814–1816 (1999).
9. T. Simpson, A. Gavrielides, and P. Peterson, "Extraction characteristics of a dual fiber compound cavity," Opt. Express **10**, 1060–1073 (2002).
10. A. Shirakawa, T. Saitou, T. Sekiguchi, and K. Ueda, "Coherent addition of fiber lasers by use of a fiber coupler," Opt. Express **10**, 1167–1172 (2002).
11. D. Sabourdy, V. Kermène, A. Desfarges-Berthelemot, L. Lefort, A. Barthélémy, C. Mahodaux, and D. Pureur, "Power scaling of fibre lasers with all-fibre interferometric cavity," Electron. Lett. **38**, 692–693 (2002).
12. D. Sabourdy, V. Kermène, A. Desfarges-Berthelemot, L. Lefort, A. Barthélémy, P. Even, and D. Pureur, "Efficient coherent combining of widely tunable fiber lasers," Opt. Express **11**, 87–97 (2003).
13. H. Bruesselbach, D. Jones, M. Mangir, M. Minden, and J. Rogers, "Self-organized coherence in fiber laser arrays," Opt. Lett. **30**, 1339–1341 (2005).
14. H. Bruesselbach, M. Minden, J. Rogers, D. Jones, and M. Mangir, "200W Self-Organized Coherent Fiber Arrays," in *2005 Conference on Lasers and Electro-Optics (CLEO)*, vol. 1, p. 532 (2005).
15. A. Ishaaya, N. Davidson, L. Shimshi, and A. Friesem, "Intracavity coherent addition of Gaussian beam distributions using a planar interferometric coupler," Appl. Phys. Lett. **85**, 2187–2189 (2004).
16. Q. Peng, Z. Sun, Y. Chen, L. Guo, Y. Bo, X. Yang, and Z. Xu, "Efficient improvement of laser beam quality by coherent combining in an improved Michelson cavity," Opt. Lett. **30**, 1485–1487 (2005).

#106878 - $15.00 USD Received 28 Jan 2009; revised 3 May 2009; accepted 5 May 2009; published 20 May 2009

17. B. Lei and Y. Feng, "Phase locking of an array of three fiber lasers by an all-fiber coupling loop," Opt. Express **15**, 17114–17119 (2007).
18. D. Mehuys, K. Mitsunaga, L. Eng, W. Marshall, and A. Yariv, "Supermode control in diffraction-coupled semiconductor laser arrays," Appl. Phys. Lett. **53**, 1165–1167 (1988).
19. D. Sabourdy, A. Desfarges-Berthelemot, V. Kermène, and A. Barthélémy, "Coherent combining of Q-switched fibre lasers," Electron. Lett. **40**, 1254–1255 (2004).
20. J. Rogers, S. Peleš, and K. Wiesenfeld, "Model for high-gain fiber laser arrays," IEEE J. Quantum Electron. **41**, 767–773 (2005).
21. W. Ray, K. Wiesenfeld, and J. L. Rogers, "Refined fiber laser model," Phys. Rev. E **78**, 046203 (2008).
22. A. Shirikawa, K. Matsuo, and K. Ueda. "Fiber laser coherent array for power scaling of single-mode fiber laser," Proc. SPIE **5662**, 482–487 (2004).
23. A. Shirakawa (personal communication, 2007).
24. P. Le Boudec, M. Le Flohic, P. Francois, F. Sanchez, and G. Stephan, "Self-pulsing in Er^{3+}-doped fibre laser," Opt. Quantum Electron. **25**, 359–367 (1993).
25. E. Lacot, F. Stoeckel, and M. Chenevier, "Dynamics of an erbium-doped fiber laser," Phys. Rev. **A 49**, 3997–4008 (1994).
26. S. Bielawski and D. Derozier, "Dynamics of a Nd-doped fiber laser: c.w. and self-pulsing regimes, stabilization," J. Phys. III France **5**, 251–268 (1995).

1. Introduction

Recognizing the power limitations of individual lasers, researchers have tried to develop methods of combining light from an array of semiconductor or fiber lasers to obtain an efficient high-power source. Extensive investigations have evaluated various coupling architectures with the goal of promoting coherent addition in the far-field of the light emitted from the output reflectors of individual lasers. Inphase array emission, where all constituent lasers operate at a common frequency and with zero relative phase difference, has been demonstrated using active control of the phases [1] and with passive coupling schemes including multicore fibers [2, 3], self-Fourier cavities [4], and Talbot resonators [5, 6]. These coupling devices often suffer from alignment issues, stability problems due to low threshold differences between array solutions, or increased cavity losses in their implementation.

An alternative approach has recently been developed to enforce coherent beam combination in arrays [7, 8, 9, 10, 11, 12, 13, 14]. In addition to a passive coupling arrangement among the elemental lasers, losses incurred at the individual output facets are purposely imbalanced. Experimental investigations have reported emission of inphase coherent light solely from the output reflector having the lowest losses. This form of single-facet emission has been studied primarily in arrays of solid-state and fiber lasers using interferometric coupling devices such as beam splitters [15, 16], fold mirrors [14], or directional couplers [8, 9, 10, 11, 13, 17]. In most realizations only one coupler output is fitted with a reflector to provide a global feedback for the entire array.

Although well-documented experimentally, few model descriptions have studied this configuration of coherent beam combining. In one depiction [9], the array of coupled lasers is treated as a single compound-cavity laser. The intrinsic laser dynamics are ignored and coherent beam combination is discussed in terms of the static eigenmodes, often referred to as supermodes, of the compound-cavity setup [18]. Although an analysis of these solutions provides important considerations necessary for inphase emission from a single output facet, the validity of this description is limited to continuous-wave (cw) emission for pump strengths very close to threshold. In contrast, experiments have shown high addition efficiency in pulsing Q-switched fiber lasers [19] and at pump strengths extending far above threshold where the output light often exhibits more complicated dynamics such as self-pulsing.

In this paper we investigate the phenomenon of coherent emission from a single output facet using an iterative map model recently introduced to describe the dynamics of fiber laser arrays [20]. Simulations of two coupled lasers with experimentally derived parameters robustly

#106878 - $15.00 USD Received 28 Jan 2009; revised 3 May 2009; accepted 5 May 2009; published 20 May 2009

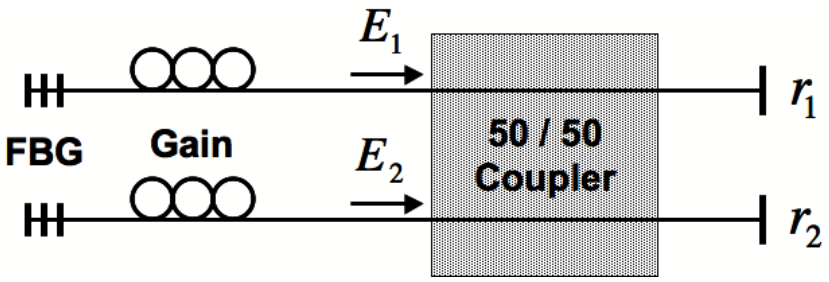

Fig. 1. Experimental schematic of two coupled lasers. Each laser gain block is terminated by a fiber Bragg grating (FBG) at one end and a high-loss output facet at the other with field reflection coefficients r_1 and r_2. A $50/50$ directional coupler allows light to interact over a small distance of the fiber lengths. The labels E_1 and E_2 indicate the frame of reference for Eq. (1).

produce coherent inphase emission of light entirely from the output facet with lowest losses, even when there is only a small mismatch in output losses [10]. Furthermore, the model shows agreement with experimental results in the presence of an additional detuning of the individual pump currents from optimal operating conditions [7, 9].

A significant feature of the iterative map model is the treatment of each individual laser as a separate dynamical oscillator influenced by the other laser via a passive, lossless coupler. Our numerical computations are consistent with a static description of the system provided by supermode theory within the latter's range of validity. In addition, the dynamical model robustly reproduces the experimental observations over a large range of pumping values spanning both cw and pulsing dynamical regimes.

2. Model description

The experiments we consider use the setup schematically illustrated in Fig. 1. Each laser cavity is formed by a fiber Bragg grating (FBG) providing nearly 100% reflection on one end and a high-loss output facet at the other end typically reflecting only about 4% of the incident intensity. A joint coupling region, most often manifested as a $50/50$ fused fiber coupler, lies between the individual gain blocks and the output facets.

2.1. Iterative maps

We recently introduced a dynamical model for a general class of fiber laser arrays which includes the setup of Fig. 1 as a special case. A set of nonlinear coupled iterative maps traces the evolution of the electric field and gain of each laser over one round trip. In a three-level lasing scheme, the forward-travelling electric fields $E_{1,2}$ and gains $G_{1,2}$ of the individual fibers, starting in Fig. 1 immediately before the output coupler, are explicitly transformed in one pass through their respective cavities over a round-trip time T according to [20, 21]

$$E_n(t+T) = e^{G_n(t)+j\phi_n^L}\sum_{\ell=1}^{2} S_{n\ell}e^{j\phi_\ell^R}r_\ell \sum_{m=1}^{2} S_{\ell m}E_m(t), \tag{1}$$

$$\begin{aligned} G_n(t+T) &= G_n(t)+\varepsilon\left[xW_{th,n}^{p}\tau\left(G_{tot}-G_n(t)\right)-\left(G_{tot}+G_n(t)\right)\right] \\ &- \frac{2\varepsilon}{I_{sat}}\left(1-e^{-2G_n(t)}\right)\,|E_n(t)|^2. \end{aligned} \tag{2}$$

#106878 - $15.00 USD Received 28 Jan 2009; revised 3 May 2009; accepted 5 May 2009; published 20 May 2009

After an initial pass through the coupler, denoted by the matrix S in Eq. (1), the emerging electric fields propagate towards the output facets with respective reflection coefficients $r_{1,2}$. The output facets are assumed to be the only source of cavity losses. The light reflected from each output face then reenters the coupler and passes through the individual gain arms before finally arriving at the starting point. The amplification of the fields due to the back-and-forth propagation through the gain sections is characterized by exponential gains $e^{G_{1,2}}$.

The round-trip time is assumed to be the same for each laser. However, small differences inevitably exist in the length and propagation constant of each cavity. At a given operational frequency, these differences are captured by assigning individual phase shifts acquired in a full round trip through each constituent laser. The phase shift acquired in each cavity over one round trip characterizes the assumed optical frequency of $E_{1,2}$. In writing these equations, we have explicitly separated the total phase shift into three parts: $\phi^L_{1,2}$ is the phase shift acquired during transit through the individual gain arms on the left-hand side of the coupler; $\phi^R_{1,2}$ denotes the phase shift picked up from propagation through the region on the right-hand side of the coupler; and the phase shift gained in the coupling region is contained in the coupling matrix S. This separation of the acquired phase shifts is important when we consider the conditions for emission from a single facet when an imbalance exists in the losses from the individual output facets. These parameters solely influence the phase shift acquired in each constituent laser as there are no nonlinearities in Eq. (1) associated with gain- or intensity-dependent phase shifts.

The evolution equation for the gain, Eq. (2), details operation of a fiber laser in a three-level scheme [21]. We adopt this form since the experiments we consider used erbium-doped fiber lasers. The relative pump rate x is the ratio of the applied pump rate to the pump rate at lasing threshold $W^p_{th,n}$. The total available gain in each laser G_{tot} is proportional to the stimulated emission cross section and obtainable population inversion. The parameter ε sets the time scale for the gain dynamics and is the ratio of the round trip time in the cavity to τ, the fluorescence time of the inversion. The saturation intensity I_{sat} dictates the average power emitting from each fiber laser. We note that although the form of Eqs. (1,2) is an accurate description of three-level operation of erbium-doped amplifying elements, the model does not capture ground-level absorption losses or pump absorption saturation effects associated with the presence of large pump and laser signals.

2.2. Coupling

Although many optical devices have been developed to couple light between individual lasers, directional couplers are often used since it is not necessary for light to enter or exit the optical waveguides in any part of the array. These evanescent couplers are typically formed by heating and pulling a packed bundle of fibers. Over an interaction region d the individual fiber cores are sufficiently narrow to release light into the shared cladding of the fiber bundle.

We have previously derived a general formulation to describe passive linear coupling for an arbitrary number of interacting fibers [20]. A directional coupler between two waveguides may be succinctly characterized by the propagation constants $\beta_{1,2}$ for light remaining within a given fiber through the coupling region and the propagation constants κ_{12} and κ_{21} describing the perturbation of light entering from the other fiber. For a symmetric coupler with $\beta_1 = \beta_2 = \beta$ and $\kappa_{12} = \kappa^*_{21} = \kappa$ (a real constant in a loss-less coupler), the coupling matrix S may be written as

$$S = e^{j\beta d} \begin{pmatrix} \cos(\kappa d) & j\sin(\kappa d) \\ j\sin(\kappa d) & \cos(\kappa d) \end{pmatrix}. \tag{3}$$

In this form it is clear that the light sloshes back-and-forth through the coupling region as a function of the interaction length. While it is difficult to experimentally determine the overall

#106878 - $15.00 USD Received 28 Jan 2009; revised 3 May 2009; accepted 5 May 2009; published 20 May 2009

phase βd acquired in the coupler, one may easily characterize κd by measuring how power entering from one fiber distributes to the two output fibers. We consider $50/50$ power splitters in this study, which requires κd to be an odd multiple of $\frac{\pi}{4}$. Any odd multiple may be used in the simulations, as other choices only differ by an overall phase shift that may be absorbed into βd.

3. Coherent beam combination

Inphase combination of light from two coupled fiber laser elements out of a single output facet was first reported by Lyndin *et al.* in 1994 [7]. Since then a number of research groups have observed this phenomenon using a variety of coupling configurations. Kozlov *et al.* enforced coherent addition between two lasers by forming a common output facet from one half of a directional coupler [8]. A majority of investigations have been performed, however, using a setup similar to the one in Fig. 1. A common output facet is selected by detuning the amount of loss incurred at the two output facets. More recent studies have shown high addition efficiencies of four, five, and even eight lasers using a hierarchical nesting of 2x2 couplers [10, 13, 22].

In this section we compare predictions of the iterative map model, Eqs. (1,2), with three features of coherent combining observed in experimental realizations of this system. The first step is to set the model parameters (see Table 1).

Table 1. Parameter values used for simulations of two coupled lasers. The operating conditions are estimated from an empirical characterization of this system found in Ref. [9].

Parameter	Description	Value	Units
T	round-trip time	163.2	*ns*
τ	fluorescence time	10	*ms*
ε	ratio of round-trip to fluorescence time	1.632×10^{-5}	dimensionless
G_{tot}	total linear gain	9.21	dimensionless
r_n	output facet reflection coefficient	varies	dimensionless
$W^p_{th,n}$	pumping at laser threshold	varies	s^{-1}
x	pumping relative to lasing threshold	varies	dimensionless
$I^{EXP,SIM}_{sat}$	saturation intensity	varies	dimensionless

3.1. Model parameters

The experimental investigations we consider were performed by two research groups using comparable setups of two fiber lasers linked by a single directional coupler. As each setup uses the same active medium with large cavity lengths, we draw information supplied by one of them to set the model parameters for all comparisons. In the experiments of Simpson *et al.* [9], two high-gain erbium-doped fibers were joined with a $50/50$ coupler and capped on the one end with high-reflecting fiber Bragg gratings. The lengths of the two fiber arms containing the gain elements were approximately 14 *m* but were not identical. One of the two coupler outputs was flat-cleaved providing a reflection of 4% of the intensity back into the cavity while the other was angle-cleaved to minimize any back reflection. Each output fiber had a length of roughly 2 *m*.

With a reported single pass gain of 40 *dB* in each active gain medium, the total linear gain parameter may be estimated as $G_{tot} = 9.21$ [9]. The round-trip time of the each cavity $T = 163.2$ *ns* is computed using an index of refraction of 1.53 and total length of 16 *m*. Taking a fluorescence time of $\tau = 10$ *ms* for each erbium-doped fiber yields an estimate of

#106878 - $15.00 USD Received 28 Jan 2009; revised 3 May 2009; accepted 5 May 2009; published 20 May 2009

$\varepsilon = 1.632 \times 10^{-5}$. As discussed in the previous section the coupling parameters must be selected to produce the power splitting effects of a $50/50$ directional coupler. Consequently we choose $\kappa = 0.001\ \mu m^{-1}$ and $d = 13351.7646\ \mu m$. Additionally, we set $\beta = 8\ \mu m^{-1}$ although this propagation constant is shared by light from both lasers and its value does not affect the output of the system.

A vast majority of the losses occur at the output facets, so the field reflection coefficients are set to be $r_1 = 0.20$ for the flat-cleaved output facet and $r_2 = 0$ for the laser with the angle-cleave. In this setup the value of ϕ_2^R does not affect the system since no light is reflected from the angle-cleaved port. Similarly the value of ϕ_1^R does not alter the dynamics because this phase shift is the same for light entering from both gain arms. Since we are free to choose these angles we set $\phi_1^R = \phi_2^R = 0$. In conrast, the choice of the phase shifts obtained during transit through the two gain arms is important. In particular, the *relative phase shift* $\Delta\phi^L = \phi_2^L - \phi_1^L$ affects the partitioning of light emitted from the two output ports in the steady state. It is important to note that the relative phase shift does not assign the transmission characteristics of a particular output port. The fraction emitted from each output port is instead influenced by the imbalance of the facet reflection coefficients. We observe that $\Delta\phi_L$ must be equal to an odd multiple of π to achieve emission from only one output facet so we set $\phi_1^L = \pi$ and $\phi_2^L = 0$.

In the following comparisons, the experimental and simulated outputs of the coupled laser system are evaluated relative to the output of a single laser member. The single laser intensity generated from model computations is matched via assignment of I_{sat} to the corresponding single laser experimental measurements over the investigated range of input pumping. The value of $W_{th,n}^p$ is taken to be the same for both lasers, but its value depends on the particular experimental investigation being simulated. Specifically, one investigation reports single laser results of an individual (uncoupled) laser while the other reports results when one laser in the coupled array is pumped. With matched single laser results, the experimental and predicted outputs of the coupled system can then be quantitatively compared under a variety of pump rates and operating conditions. This method of evaluation also allows access to metrics commonly used to assess the overall performance of coherently combined laser systems. One metric we will use is the addition efficiency, an estimation of the fraction of light emitted from each output port compared to the sum of the outputs of the uncoupled lasers.

(It is also necessary to make comparisons in this manner because the experimental measurements are reported in terms of emitted powers or voltages from detection equipment. Since efficiencies of the pump or detection electronics are not given, we cannot directly calibrate the output of our model with the recorded experimental results.)

3.2. Power extraction

We first examine coherent combining in a symmetrically pumped array of two lasers. Figure 2(a) depicts experimental power extraction measurements performed by Shirakawa *et al.* for increasing levels of the pump [23]. For reference the solid line plots the power output characteristics of a single fiber laser detached from the coupler with a flat-cleaved output facet. The pumping is reported relative to lasing threshold of the single laser and the intensity is divided by the average intensity of the laser measured at a pump value of 50 times the lasing threshold. In the case of two coupled lasers, the power extracted from the two output ports is displayed by the circles in Fig. 2(a). The filled circles represent the average intensity emanating from the flat-cleaved output facet associated with the first laser, while the open circles depict the average intensity from the very high-loss angle-cleaved output facet of the second laser. We see that almost all light emits from the flat-cleaved output facet with the lowest losses, and no light is observed from the angle-cleaved output facet. Comparison with the individual laser extraction shows that, although both have the same lasing threshold, the slope efficiency of the

#106878 - $15.00 USD Received 28 Jan 2009; revised 3 May 2009; accepted 5 May 2009; published 20 May 2009

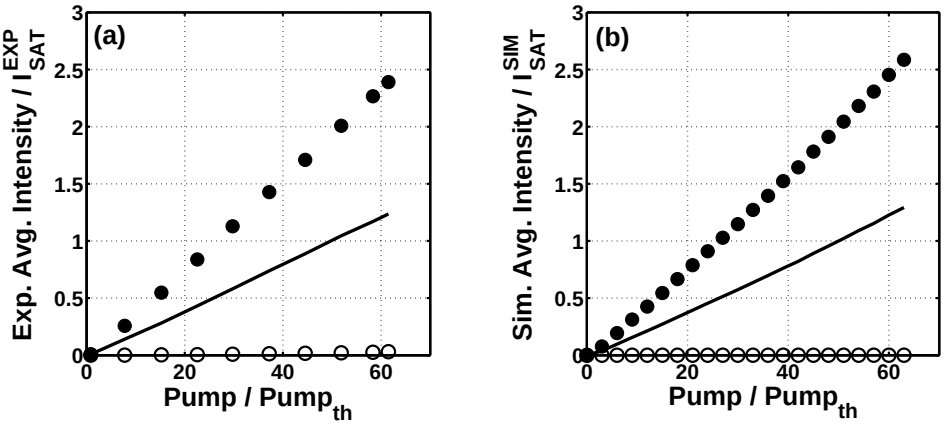

Fig. 2. Power output characteristics for individual and two coupled lasers with imbalanced losses at the output facets. The solid line represents the average intensity produced by a single laser removed from the array. The filled (open) circles represent the average intensity output from the low (high) loss output facet for two coupled and symmetrically pumped lasers. (a) Experiment using two coupled erbium-doped fiber lasers [23]. (b) Simulation using iterative map model. For (a) and (b) the pumping is taken relative to lasing threshold for a single, uncoupled laser. The intensity axis in each panel is taken relative to $I_{sat}^{EXP,SIM}$, the respective single laser intensity at 50 times the lasing threshold.

symmetrically pumped lasers is nearly twice that of the single laser demonstrating a 93% combining efficiency [10]. The results of Fig. 2(a) are in agreement with other experimental power extraction curves showing combining efficiencies up to 99% [11].

The power extraction predicted from model computations is shown in Fig. 2(b). The solid line in this figure represents the average intensity obtained for a single uncoupled laser. Similar to the presentation of the experimental data in Fig. 2(a), the pump is shown relative to pump threshold and the intensity is taken relative to emission at 50 times the lasing threshold. Model simulations indicate that $W_{th,n}^{p} = 1.4235$ and $I_{sat}^{SIM} = 473.45$ for an individual laser. The circles in Fig. 2(b) plot the predicted outputs of the modeled array. The filled (open) circles represent the average intensity emitting from the output port with lower (higher) losses. In the simulation emission from the flat-cleaved port completely dominates the output with an addition efficiency of 100%.

It is worthwhile to point out that efficient coherent beam combination is observed in the model computations regardless of the time-resolved intensity dynamics predicted for the system. In particular, for both coupled and uncoupled lasers, emission in the cw state is observed only at pump strengths in the range $1 < x < 1.1255$ above threshold. The intensity and gain dynamics exhibit self-pulsing at higher relative pump rates. As the pump is further increased the height and frequency of the pulses rise linearly while the width of an individual pulse decreases. Although not all fiber laser systems suffer from the self-pulsing instability, it most often appears at pump levels near threshold in high-gain fiber lasers operated with heavy cavity losses [24, 25, 26]. However, the underlying dynamical state does not affect time-averaged extraction curves from single or coupled lasers because the time-averaged intensity of a pulse train is identical to the value of the unstable cw state at a given pump rate [21].

#106878 - $15.00 USD Received 28 Jan 2009; revised 3 May 2009; accepted 5 May 2009; published 20 May 2009

3.3. *Detuning of the pump sources*

In the previous section the lasers were operated in a symmetrical fashion, including equal levels of pumping applied to each fiber arm. We now examine what happens when there is a mismatch in the individual pump strengths. For comparison in Fig. 3(a) we reproduce the data shown in Fig. 4 of Ref. [9], an experimental realization of two extractions where one laser is fixed to a particular pump value and the pump strength of the second laser is detuned around the fixed value.

The first extraction measurement involves setting the pump strength of the first laser to zero and increasing the pump strength of the second laser. The solid line in Fig. 3(a) plots the time-averaged output obtained from the flat- and angle-cleaved output ports. In this case the intensity emitted from each output port is the same at all pump levels since light amplified in a single gain arm is split evenly in the $50/50$ coupler. This extraction serves as a reference for the output of a single laser, although this component laser incurs more losses than an individual (uncoupled) laser due to the presence of the coupler in the laser cavity. The pump strength is reported here relative to the observed lasing threshold and the intensity is taken relative to the emission from one of the output ports when the component laser is pumped at twice the lasing threshold.

For the second experimental extraction measurement, the pump strength of the first laser is set to 1.52 times the lasing threshold of the component extraction curve and the second laser is tuned from 0 to 2.2 times lasing threshold. In Fig. 3(a) the filled circles represent time-averaged emission from the flat-cleaved output facet while the open circles depict the intensity from the angle-cleave of the second laser. When the second laser pump is less than 0.9 times the component lasing threshold, the two output facets emit at equal intensity levels. At higher pump strengths the flat-cleaved light output is seen to increase linearly while the angle-cleaved output tends toward zero. After the pump of the second laser is raised above the fixed pump level of the first laser, the intensity emerging from the angle-cleaved output is observed to increase.

Figure 3(b) shows the corresponding extraction curves we find from simulations of Eqs. (1,2). As in the experiment, we first fix the pump of one laser to zero and sweep the second laser pump until about twice the observed lasing threshold. The simulations similarly predict an equal level of emission from the flat- and angle-cleaved output ports over the range of the second laser pump. This sweep yields the assignment of $W^p_{th,n} = 1.6667$ and $I^{SIM}_{sat} = 144.83$ for the component laser. All other model parameters remain as before. The solid line in Fig. 3(b) plots the scaled simulated extraction.

The second power extraction is computed by setting the pump of the first laser to 1.52 times the component lasing threshold and sweeping the pump of the second laser. The relative pump rate of the first laser is high enough that the intensity dynamics are in the pulsing regime for all investigated pump levels of the second laser. The filled circles in Fig. 3(b) represent emission from the output port terminated by a flat-cleave and the open circles show the intensity from the angle-cleave. It is immediately clear that the intensity from the angle-cleaved port follows a trend similar to the experimental measurement. A minimum in this output is realized when the two laser pumps are identical.

The emergence of light from the angle-cleaved output port in this extraction can be explained by a linear analysis of interference in the $50/50$ coupler [12]. When light from back-reflection off the output port splits equally into the two gain sections, the intensities are magnified by different amounts. Following amplification, the contrast of the imbalanced intensities reentering the coupler towards the output reflector results in incomplete destructive interference into the angle-cleaved output port.

It is apparent in Fig. 3 that the simulated extraction demonstrates a higher degree of coherent combining than the experimentally reported extraction at all considered pump levels. The inefficient beam combining observed in the experiment is due to internal losses of light not

#106878 - $15.00 USD Received 28 Jan 2009; revised 3 May 2009; accepted 5 May 2009; published 20 May 2009

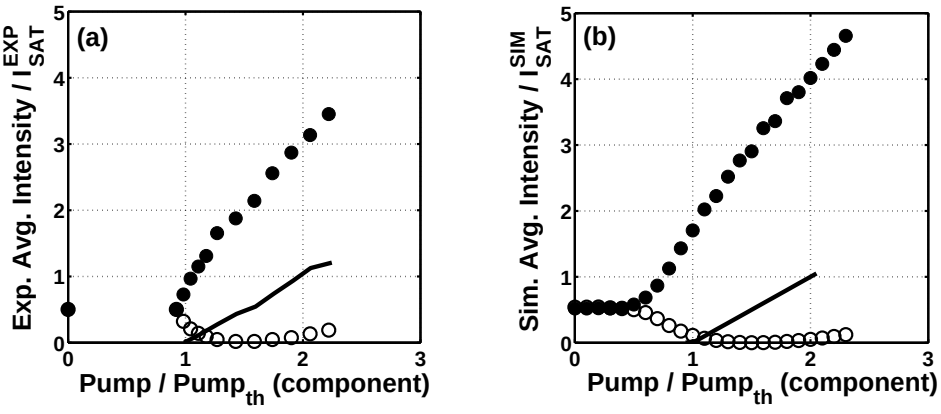

Fig. 3. Average intensity output for two coupled lasers with imbalanced losses at the output facets and asymmetrical diode pumping levels. The solid line in each panel plots the extraction emitted from both the lower- and higher-loss ports when only one component laser is pumped. The circles plot the extraction when the first laser is fixed at 1.52 times lasing threshold while the second is swept from 0 to 2.3 times lasing threshold. In each plot the filled (open) circles represent the average intensity emission from the lower (higher) loss output facet of the two lasers. (a) Reproduction of experimental data from Fig. 4(a),(b) of Ref. [9]. (b) Simulation using our iterative map model. For (a) and (b) the pumping is taken relative to lasing threshold where only one component laser in the array is pumped. The intensity axis in each panel is taken relative to the respective single laser intensity at twice the component lasing threshold.

considered in the model [9] as well as non-ideal interference of the light at the coupler. An additional discrepancy in the extractions is the sub-threshold value of the relative pump rate where the average intensity emitting from the two output ports begins to split. The split in the output power from each facet results from interference in the coupling region of light entering in from the two laser arms. In the simulation this occurs at 0.5 times the component lasing threshold, a much lower value than the experimentally observed level. This difference arises because the model equations do not account for mechanisms in the under-pumped laser that extinguish light entering from the other laser. Contributing factors include ground-level absorption and inefficiencies in pump absorption due to the presence of the laser light coupled in from the pumped cavity.

3.4. Detuning of the output facet losses

So far we have investigated a special case of imbalanced losses at the two output facets. Namely, there is only a single output facet providing feedback of light to the two cavities; the other port is angle-cleaved so that effectively all approaching light is transmitted out of the system. In essence this is a single compound-cavity laser with a shared output facet and it is unclear that the two lasers in the model need be viewed as two separate but coupled oscillators.

On the other hand, a recent experimental investigation of two coupled erbium-doped fiber lasers demonstrated that coherent addition of light from a single output port is a general phenomenon which emerges even when the field reflection coefficients of the two output ports are only slightly different [10]. This laser array is identical to the one considered in Section 3.2 except the two output facets exhibit only slightly different cavity losses. At a fixed level of

#106878 - $15.00 USD Received 28 Jan 2009; revised 3 May 2009; accepted 5 May 2009; published 20 May 2009

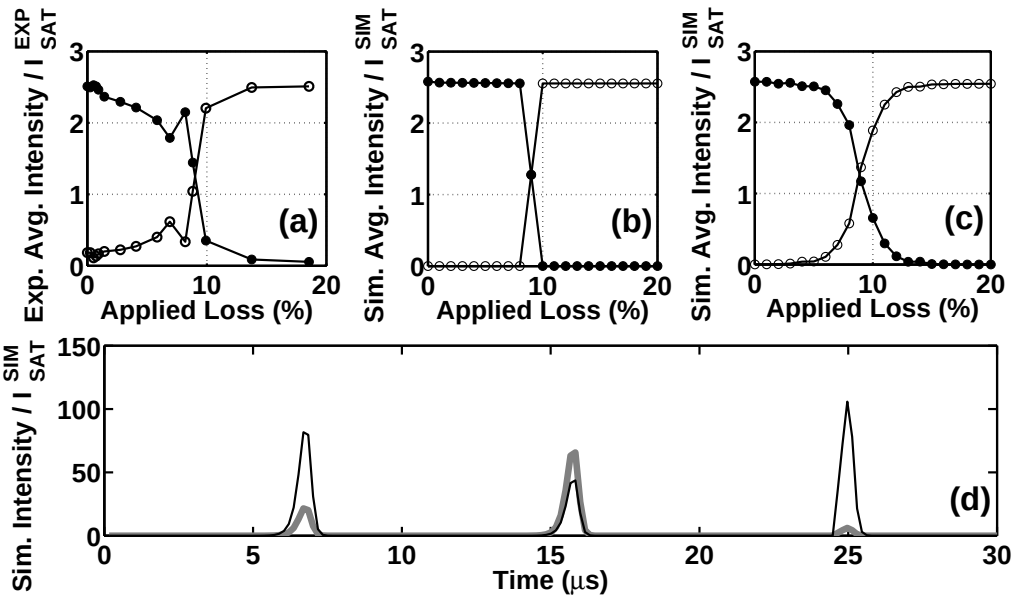

Fig. 4. (a)-(c) Plot of average intensity output as a function of the applied losses at the output facet of the first laser. The losses of the second laser are 9% higher than the losses of the first laser without applied losses. The filled (open) circles show the average intensity measured from the first (second) laser. Data shown for (a) experiment [reproduction of Fig. 4 from Ref. [10]] (b) simulation without noise (c) simulation with noise. (d) Intensity time trace from simulation with noise for applied loss level of 8%. The thin (thick) line plots pulses from first (second) laser. Values of $I_{sat}^{EXP,SIM}$ represent the experimental and simulated single laser intensity at 50 times the lasing threshold.

identical pumping in each constituent laser, the losses in the lower-loss output arm were gradually increased until the total loss in this fiber port exceeded those of the other output facet. The observed average intensity from each output facet is displayed in Fig. 4(a) as the applied loss in the lower-loss arm (filled circles) is increased from 0% to 20%. The losses in the second fiber port (open circles) are fixed at a level of 9% higher than the lower-loss fiber port without applied loss. For a large detuning between the losses in output arms, the entirety of the emitted light was seen to reside in the output port with the lowest level of loss. Close to the transition point at 9% applied loss, the power measurements were unstable and light emerged from both output facets.

To replicate this experiment, we use the same model parameters as in Section 3.2 except that we now use one of the reflection coefficients as a control parameter. In particular, we leave $r_1 = 0.2$ for the flat-cleaved output face and now set $r_2 = 0.1908$ to produce a 9% greater loss of intensity at the output face. Since the reflection coefficient of the second laser is now nonzero, the assignment of ϕ_2^R is no longer trivial. Nevertheless, when $\Delta\phi^L = \pi$ the choice of ϕ_1^R and ϕ_2^R does not affect the outcome of the simulations. We again arbitrarily set $\phi_1^R = \phi_2^R = 0$. The simulated pump level is set to 62.5 times the lasing threshold for an individual (uncoupled) laser to match the average intensity measured in the experiment. At this pumping the intensity dynamics of the model exhibit irregular self-pulsations.

In Fig. 4(b) we plot the simulation results as r_1 is decreased from 0.2 to 0.179, representing a 20% increase in the losses from this output port. The filled (open) circles represent the intensity emitted from the output facet of the first (second) laser. There is excellent agreement with

#106878 - $15.00 USD Received 28 Jan 2009; revised 3 May 2009; accepted 5 May 2009; published 20 May 2009

Fig. 4(a), and a sharp transition in the emission characteristics occurs once the losses in the first laser are greater than 9%. When the losses between the two lasers differ by less than 1%, the transients of the intensity in the simulations are very long but eventually the system settles down to emission from just one output port.

The unstable emission characteristics experimentally observed in the transition region may be captured by the addition of a small amount of Langevin noise to the electric field map Eq. (2). Figure 4(c) plots the average intensity measured from each output facet for a noise amplitude of 0.02. The addition of noise provides a smoothing effect in the transition region and one output facet is no longer completely dominant. In Fig. 4(d) we show a simulated intensity time series for an applied loss of 8%. The thin (thick) line denotes the intensity from the first (second) laser. The first laser emits a majority of the system output. The light from the second laser behaves more erratically and the pulses occasionally reach higher intensities than those emitting from the first laser.

4. Discussion: static vs. dynamic perspectives

The coherent addition of lasers observed in these kinds of experiments is traditionally interpreted within a static framework of coupled optical waveguides without any regard to the amplification of the light in the gain medium. The stripped-down coupled cavity is then treated as a single entity, and the resulting eigenmodes of the system, sometimes called supermodes, are then analyzed as the basis to describe the observed dynamics in the laser. It is typically postulated that the lowest loss supermode will "win" by emerging as the stable state, although growth or decay of individual eigenmodes are rarely quantified.

For example, when two coupled lasers are identical except for an imbalance in the output facet reflection coefficients, it is intuitive that losses can be minimized if all of the light is funneled to the output port with the higher reflectivity. When the cavity conditions are specified such that the light propagating back-and-forth through the two (now passive) gain arms capped with 100% reflectors pick up a relative phase shift of π, then two constructive supermodes result which funnel light to either one or the other output port [10]. The supermode associated with the lower-loss output port retains more light each round-trip and consequently will be selected by the laser system. In fact, this supermode will be globally selected over other supermodes formed from other cavity configurations where the relative phase shift in the gain arms is not equal to π, since for these non-optimal relative phase shifts light will invariably be funneled to the higher-loss port.

The current description offers an alternative to this static perspective. We have shown that including gain as a dynamical variable and treating each laser as a separate oscillator does equally well at predicting the experimentally observed behavior in the linear (cw) regime. Preferential emission from the lowest-loss output port is a direct consequence of the dynamical interplay between the gain elements and the imbalanced losses at the output facets. In addition the dynamical model also extends correct predictions far beyond threshold and even into the pulsing regime. Indeed, the coupling between the two lasers tends to align the pulse bursts of the individual lasers so that constructive interference is achieved in the coupler at all times.

It is natural to ask about the robustness of the theory with respect to inevitable imperfections, for example in the coupler. We tested this by repeating all of the simulations using a 49/51 coupler; in all cases the new numerical data lie extremely close to the old. Roughly speaking, the effects appear to vary as the square of the mismatch from $50/50$ coupling: for example, in the extraction plot shown in Fig. 2 the amount exiting from the angle cleave is less than 0.1% of the light of the individual laser (no light exits the angle cleave in the $50/50$ coupler).

Although this model reveals a mechanism for selecting which of the two output ports (supermodes) receives a larger share of the light, it does not explain in a fundamental sense the

#106878 - $15.00 USD Received 28 Jan 2009; revised 3 May 2009; accepted 5 May 2009; published 20 May 2009

relative amount of light emitted from each. This partitioning depends only on the value of $\Delta\phi^L$, a manually set parameter in this model, and we have fixed $\Delta\phi^L = \pi$ to simulate the nearly complete beam-combining observed experimentally. Even though multiple thousands of longitudinal modes may potentially oscillate in a fiber laser, only some of these are characterized by this value of $\Delta\phi^L$. A direction of future research would be the extension of this model to a multimode framework allowing simultaneous oscillation of modes characterized by different $\Delta\phi^L$. Competition among these modes may shed light on the dynamical selection of frequencies associated with this optimal relative phase shift. Additionally, from this groundwork the influence of optical nonlinearities relevant at higher powers, such as stimulated Brillion scattering and stimulated Raman scattering, may be directly assessed by appropriate extensions of the model. These observations demonstrate the importance of a dynamical model in developing an understanding of organized behavior in coupled laser systems.

Acknowledgment

We thank Akira Shirakawa for valuable discussions and providing his original data for our use. This work was supported by the High Energy Laser Joint Technology Office and the US Army Research Office under Award No. W911NF-05-1-0506. Any opinions, findings, and conclusions or recommendations expressed in this publication are those of the authors and do not necessarily reflect the views of the High Energy Laser Joint Technology Office or the Army Research Office.

#106878 - $15.00 USD Received 28 Jan 2009; revised 3 May 2009; accepted 5 May 2009; published 20 May 2009